High Energy Physics and Nuclear Physics

Volume 12, No. 3

A Wide-Range Magnetic Spectrometer For Electron Scattering In Medium Energy Range*

Mao Zhenlin

(Institute of High Energy Physics, Chinese Academy of Sciences, Beijing)

A non-focusing magnetic spectrometer designed for electron scattering in medium energy region is proposed. The positions read out from the position-sensitive detectors in the spectrometer are used for track reconstruction and momentum measurement through a computer program. The structure of this spectrometer is rather simple and no special technique and element are required for the correction to aberration. It is suitable for the usage of a spectrometer with a large solid angle and wide momentum range. The momentum resolution, momentum range, and acceptance in our case are calculated by Monte Carlo simulation.

1. INTRODUCTION

The electron scattering by nuclei and nucleons plays an important role in the study of nuclear and nucleonic structure. The injector of the Beijing Electron and Positron Collider (BEPC) [1] is an electron linac with an energy of 1.4 GeV. The electron beam from this linac can be used in many aspects of the electron scattering [2], such as: (1) delta-isobar induced by the electrons in nuclei; (2) studies of longitudinal and transverse response functions and Y-scaling in the quasi-elastic region; (3) measurements of form factors for some light nuclei ($A \leq 4$) in the large Q^2 region.

In order to meet the needs of the above experiments, the specifications of the magnetic spectrometer are selected as follows: momentum resolution ≤ (1–2)%, solid angle = 1–4 msr, momentum acceptance P_{max}/P_{min} = 1.5–2.0.

* Project supported by the National Natural Science Foundation of China
Received on February 5, 1987

So far the magnetic spectrometers designed for the electron scattering in medium energy range are of focusing type only. Some of the spectrometers have single dipole structure (D) [3], others have double dipole structure (DD) [4] or even more complicated structure [5]. The specifications of all these magnetic spectrometers are within the range of $10^{-3}-10^{-4}$ for momentum resolution, 1–17 msr for solid angle and $P_{max}/P_{min} = 1.1-1.5$ for momentum acceptance.

In order to obtain the focusing condition for a focusing type magnet, a larger object distance should be selected for medium energy electrons, because it is proportional to the radius of the curvature of the particle in the magnetic field. If we need a larger solid angle at the same time, a larger aperture of the magnet has to be selected and the aberration has to be corrected very carefully as well. Thus, such magnet even with smaller momentum acceptance is still very large, precise, and expensive.

A non-focusing magnetic spectrometer designed for larger momentum acceptance with single dipole structure (D) is proposed in this paper. The positions of the particle recorded by the detectors located at the front and the back of the magnet can be used to determine the trajectory and momentum of the particle through computer programs. The construction of this spectrometer is rather simple, no special element is needed for the correction to aberration and it is cheaper. A calculation by Monte Carlo simulation in our case shows that the momentum resolution $\Delta P/P = 0.16\%$ (FWHM), solid angle $\Omega = 3.6$ msr and momentum acceptance $P_{max}/P_{min} = 1.7$ can be obtained for such a magnetic spectrometer at deflecting angle $\alpha = 50°$.

2. PRINCIPLE AND FORMULAS

A non-focusing spectrometer with single D structure is shown in Fig. 1a, where T is the target. A particle ejected from a target point $P_0(x_0,\theta_0,y_0,\phi_0)$ goes through the multiwire proportional chamber MWPC at $P_1(x_1,\theta_1,y_1,\phi_1)$ and enters the magnet M. The positions of the particle at the entrance and the exit of the magnet are $P_2(x_2,\theta_2,y_2,\phi_2)$ and $P_3(x_3,\theta_3,y_3,\phi_3)$ respectively. Then the particle goes through two multiwire drift chambers MWDC1 and MWDC2, and through the scintillation counter S consecutively, then finally enters the shower counter S.D.. The positions of the particle at the two drift chambers are $P_4(x_4,\theta_4,y_4,\phi_4)$ and $P_5(x_5,\theta_5,y_5,\phi_5)$ respectively. The position parameters, x_1, x_4, y_4, x_5, y_5, read out by the multiwire proportional chamber and multiwire drift chambers can be used to determine the deflecting radius of the particle in the magnetic field through a computer program, the momentum of the particle is thus determined. The lead glass shower counter S.D. is used for particle identification, and the signal from the scintillation counter together with the beam pulse will be the trigger for the data acquisition system.

The coordinate system and the meaning of the notations of the positions $P_i(x_i,\theta_i,y_i,\phi_i)$, $i = 1,2,...5$ described above are the same as that in Ref.[6]. The direction of the motion of the particles on the central trajectory is designated as coordinate z, and the direction of the deflecting force by magnetic field to the particles on the central trajectory is designated as coordinate x. Coordinate y is perpendicular both to coordinate x and coordinate z. An arbitrary trajectory of a particle is denoted by $P_i(x_i,\theta_i, y_i, \phi_i)$, where (x_i,y_i) represent the positions of the particle at this coordinate system, and (θ_i, ϕ_i) represent the

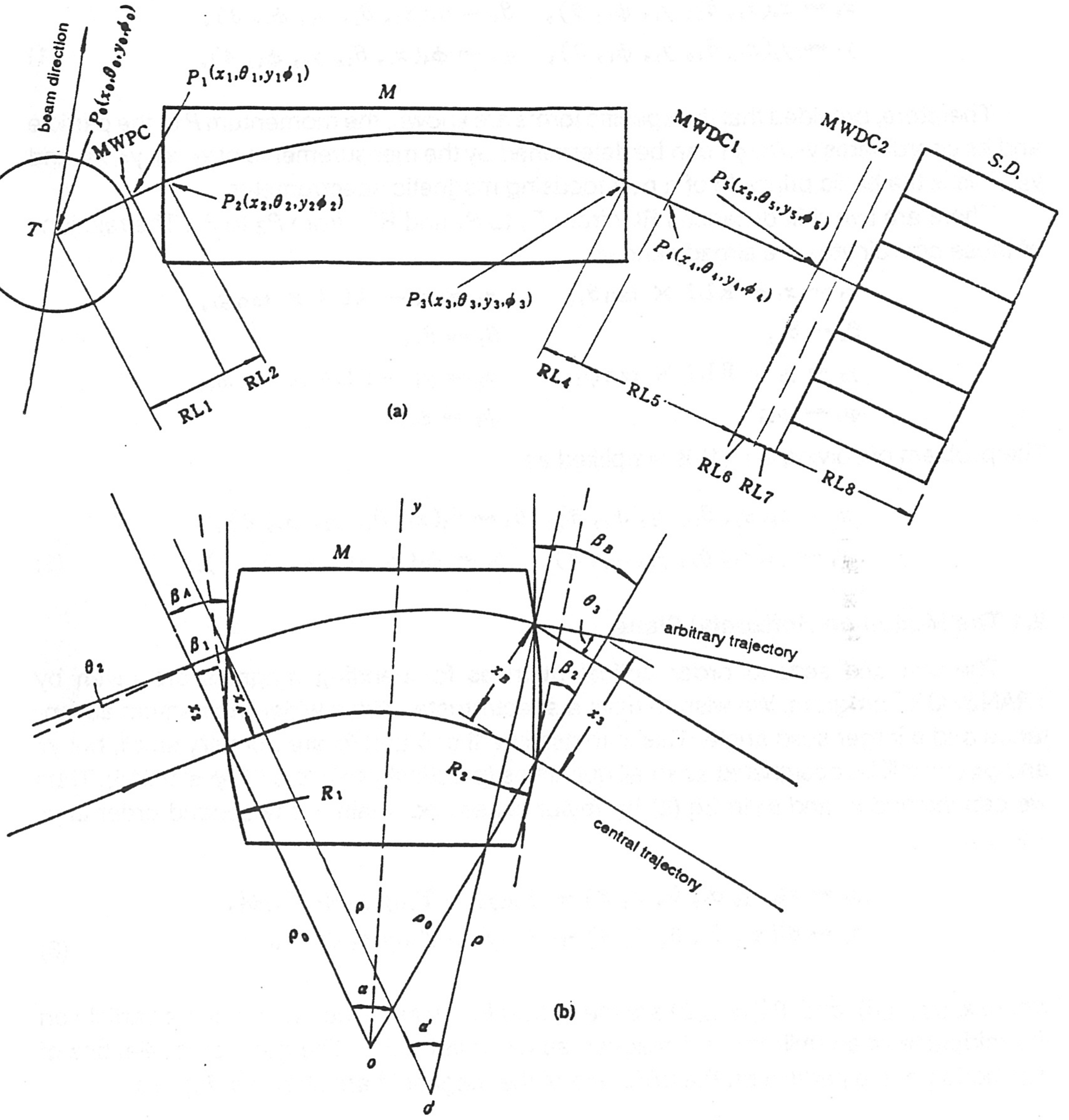

FIG. 1 (a) The sketch of the non-focusing magnetic spectrometer with single D structure. (b) The geometric relations of the particle's motion at midplane of the magnet M.

angles of the projections of the particle's trajectory on the x_iz and y_iz plane with the z axis respectively.

In general, the position coordinates $P_4(x_4,\theta_4,y_4,\phi_4)$ of a particle after going through the magnetic field are determined by the position coordinates $P_1(x_1,\theta_1,y_1,\phi_1)$ of the particle before entering the magnetic field and its momentum P (sometimes replaced by fractional deviation of momentum $\delta = (P - P_0)/P_0$):

$$x_4 = x_4(x_1, \theta_1, y_1, \phi_1, \delta), \quad \theta_4 = \theta_4(x_1, \theta_1, y_1, \phi_1, \delta),$$
$$y_4 = y_4(x_1, \theta_1, y_1, \phi_1, \delta), \quad \phi_4 = \phi_4(x_1, \theta_1, y_1, \phi_1, \delta). \tag{1}$$

Therefore, provided that the specific forms are known, the momentum P of the particle and its coordinates y_1, θ_1, ϕ_1 can be determined by the measurements of x_1, x_4, y_4, x_5, and y_5. This is the basic principle of a non-focusing magnetic spectrometer.

There are two drift distances RL2 from P_1 to P_2 and RL4 from P_3 to P_4. The relations of these coordinates are already known,

$$\begin{aligned} x_2 &= x_1 + \mathrm{RL2} \times \tan\theta_1, & x_3 &= x_4 - \mathrm{RL\,4} \times \tan\theta_4, \\ \theta_2 &= \theta_1, & \theta_3 &= \theta_4, \\ y_2 &= y_1 + \mathrm{RL2} \times \tan\phi_1, & y_3 &= y_4 - \mathrm{RL\,4} \times \tan\phi_4, \\ \phi_2 &= \phi_1; & \phi_3 &= \phi_4. \end{aligned}$$

The problem of solving Eq. (1) is simplified as

$$x_3 = x_3(x_2, \theta_2, y_2, \phi_2, \delta), \quad \theta_3 = \theta_3(x_2, \theta_2, y_2, \phi_2, \delta),$$
$$y_3 = y_3(x_2, \theta_2, y_2, \phi_2, \delta), \quad \phi_3 = \phi_3(x_2, \theta_2, y_2, \phi_2, \delta). \tag{2}$$

2.1 The Motion on Horizontal Plane

The first and second order optical matrixes for bending magnets are given by TRANSPORT program. We wish to have a spectrometer with a wider momentum acceptance and a larger solid angle. This is to assume that δ and θ_2 are not very small, but y_2 and ϕ_2 can still be designated as small quantities (practically $y_2/\rho \le 0.02, \phi \le 0.015$). Thus we can expand x_3 and θ_3 in Eq.(2) by Taylor series and retain to the second order of y_2 and ϕ_2:

$$x_3 = x_3^0(x_2, \theta_2, 0, 0, \delta) + T_{133}y_2^2 + T_{134}y_2\phi_2 + T_{144}\phi_2^2,$$
$$\theta_3 = \theta_3^0(x_2, \theta_2, 0, 0, \delta) + T_{233}y_2^2 + T_{234}y_2\phi_2 + T_{244}\phi_2^2. \tag{3}$$

where $x_3^0(x_2,\theta_2,\delta)$ and $\theta_3^0(x_2,\theta_2,\delta)$ are the optical formulas of the motion of the particle on the midplane of an uniform-field magnet, as given in Ref.[7]. The geometric relations of the motion of the particle on the midplane of the magnet M are shown in Fig. 1b.

$$\begin{aligned} \theta_3^0 &= \beta_B + \sin^{-1}\left[\sin(\alpha + \theta_2 - \beta_B) - \frac{2\rho_0}{\rho}\sin\frac{\alpha}{2}\cos\left(\frac{\alpha}{2} - \beta_B\right) \right. \\ &\quad \left. - \frac{x_A}{\rho\cos\beta_A}\sin(\alpha - \beta_A - \beta_B)\right], \\ x_B &= \rho\cos\theta_3^0 - \rho\cos(\alpha + \theta_2) - \rho_0(1 - \cos\alpha) + \frac{x_A}{\cos\beta_A}\cos(\alpha - \beta_A), \\ x_2 &= x_A(1 - \tan\theta_2\tan\beta_A), \\ x_3^0 &= x_B(1 + \tan\theta_2\tan\beta_A), \\ \beta_1 &= \beta_A - \sin^{-1}\frac{x_A}{2R_1\cos\beta_A}, \\ \beta_2 &= \beta_B - \sin^{-1}\frac{x_B}{2R_2\cos\beta_B}. \end{aligned} \tag{4}$$

we can get x_3^0 and θ_3^0 from, x_2, θ_2, ρ by formula (4).

The magnetic field is assumed to be sharp cut-off in deriving formula (4). That is called sharp cut-off approximation (SCOFF). In practice, the magnetic field decreases slowly by a gradual descent. It was shown in Ref.[8] that the result of the deflecting angle for a particle going through the uniform-field on the midplane calculated by the equivalent boundary sharp cut-off approximation is identical to the calculated result with an extended edge field (EFF). If we coincide the EFF trajectory with the SCOFF trajectory in the uniform field region, the displacements of these trajectories are $\Delta x_1 = g^2 I_1/\rho\cos^2\beta_1$ and $\Delta x_2 = g^2 I_1'/\rho\cos^2\beta_2$ at the entrance and the exit of the magnet respectively, where I_1 and I_1' are determined by the actual distribution of the extended edge field. In general, I_1, $I_1 < 1$, g is the air gap of the magnet. These formulas give the corrections for the extended edge field.

The formulas of the second order coefficients T_{ijk} with EFF corrections were also given in Ref.[8].

2.2 The Motion on the Vertical Plane

The formulas of the first and second order coefficients with EFF corrections can be written by matrix equation:

$$\begin{bmatrix} y_3 \\ \phi_3 \end{bmatrix} = \begin{bmatrix} 1 & x_3\tan\beta_2 \\ 0 & 1 \end{bmatrix}\begin{bmatrix} 1 & 0 \\ -1/f_2 & 1 \end{bmatrix}\begin{bmatrix} 1 & L \\ 0 & 1 \end{bmatrix}\begin{bmatrix} 1 & 0 \\ -1/f_1 & 1 \end{bmatrix}\begin{bmatrix} 1 & x_2\tan\beta_1 \\ 0 & 1 \end{bmatrix}\begin{bmatrix} y_2 \\ \phi_2 \end{bmatrix}, \qquad (5)$$

where $1/f_1$ and $1/f_2$ are the effective lens strengths at the entrance and exit edges of the magnet respectively. L is the length of an arbitrary trajectory.

$$F_1 = \frac{1}{f_1} = \frac{\tan\beta_1'}{\rho},$$

$$F_2 = \frac{1}{f_2} = \frac{\tan\beta_2'}{\rho},$$

$$L = \alpha'\rho_0$$

and

$$\beta_1' = \beta_1 + \theta_2 - \frac{x_1}{R_1\cos\beta_1} - \frac{gI_2(1+\sin^2\beta_1)}{\rho\cos^3\beta_1},$$

$$\beta_2' = \beta_2 - \theta_3 + \frac{x_2}{R_2\cos\beta_2} - \frac{gI_2'(1+\sin^2\beta_2)}{\rho\cos^3\beta_2},$$

$$\alpha' = \alpha + \theta_2 - \theta_3,$$

where I_2 and I_2' are determined by the edge field at the entrance and exit of the magnet. Letting $L_1 = x_2\tan\beta_1$ and $L_2 = x_3\tan\beta_2$, expanding the matrix equation (5), we get

$$\begin{aligned} y_3 = {} & \{1 - F_2L_2 - F_1[(1-F_2L_2)L + L_2]\}y_2 + \{(1-F_2L_2)L_1 \\ & + (1-F_1L_1)[L_2 + (1-F_2L_2)L]\}\phi_2, \\ \phi_3 = {} & [-F_2 - F_1(1-F_2L)]y_2 + [-L_1F_2 + (1-F_2L)(1-F_1L_1)]\phi_2. \end{aligned} \qquad (6)$$

Eqs. (3), (4), and (6) are the optical formulas for the particle transferred from the entrance to the exit of the magnet.

3. DETERMINE ρ AND θ_2 FROM THE MEASUREMENTS

The coordinates x_1, x_4, y_4, x_5, y_5 can be measured by the multiwire proportional chamber and multiwire drift chambers. Then the coordinates x_3, θ_3, y_3, ϕ_3 at the exit of the magnet can be determined by x_4, y_4, x_5, y_5.

In order to deduce ρ and θ_2 from x_3, θ_3, y_3, ϕ_3 and x_1, at first we assume that the motion of the particle is at the midplane of the magnet. x_2 and θ_2 can be obtained from x_3^0, θ_3^0, x_1 by the following formulas:

$$\theta_2 = 2\beta_B - \alpha - \theta_3^0 - 2\tan^{-1}\left(\frac{B + A\sin\beta_B}{A\cos\beta_B}\right),$$

$$x_4 = x_1 + \mathrm{RL}\,2 \times \tan\theta_2,$$

where

$$A = -2\rho_0 \sin\frac{\alpha}{2}\cos\left(\frac{\alpha}{2} - \beta_B\right) - \frac{x_A}{\cos\beta_A}\sin(\alpha - \beta_A - \beta_B),$$

$$B = x_B + \rho_0(1 - \cos\alpha) - \frac{x_A}{\cos\beta_A}\cos(\alpha - \beta_A).$$

The quantity ρ can be calculated by

$$\rho = \frac{2\rho_0 \sin\frac{\alpha}{2}\cos\left(\frac{\alpha}{2} - \beta_B\right) + \frac{x_A}{\cos\beta_A}\sin(\alpha - \beta_A - \beta_B)}{\sin(\alpha + \theta_2 - \beta_B) - \sin(\theta_3 - \beta_B)}. \quad (7)$$

Interchanging $\begin{bmatrix} y_3 \\ \phi_3 \end{bmatrix}$ and $\begin{bmatrix} y_2 \\ \phi_2 \end{bmatrix}$, and also the subscripts 1 and 2 of other variables, Eq. (6) still holds. Substituting ρ from (7) to inverse functions of (6), we can get y_2 and ϕ_2, and also we can calculate the second-order coefficients T_{ijk}, then the new values of x_3^0 and θ_3^0 can be obtained from (3). From x_1 and the new values of x_3^0, θ_3^0 we can get ρ and θ_2 again. The calculation is iterated until the difference between the successive two ρ's is less than a given error.

Then the momentum of the particle can be determined by $P = (\rho/\rho_0)P_0$, where P_0 and ρ_0 are the central momentum and central radius respectively.

4. A MONTE-CARLO-SIMULATED CALCULATION FOR THE SPECTROMETER

Magnet M of the spectrometer shown in Fig 1 (a) will be rebuilt with a MA type deflecting magnet which was used in the beam line of DESY 7 GeV synchrotron. After rebuilding the parameters of the magnet are expected as follows: maximum magnetic field 18 kG, air gap 6 cm, effective length 132.7 cm and the width of the uniform-field region 36 cm. The deflecting angle α of the central trajectory can be adjusted according to the desire of the experimenters, but we set $\beta_1 = \beta_2 = \alpha/2$ for better focusing at y direction.

The position resolutions of the multiwire chamber and multiwire drift chamber are designed to be 0.5 mm and 0.2 mm respectively. In order to reduce the angular uncertainty of the particles induced by multiple scattering, two helium bags with 1 atm pressure will be inserted between MWPC and two MWDCs.

The uncertainty of θ_4 induced by position uncertainties of MWDC1 and MWDC2 is about 0.03°. The total thickness of the material from MWPC to MWDC2 is about 10^{-3} radiation length. Estimated angular uncertainty by multiple scattering is 0.02° at particle's momentum of 800 MeV/*c*. The momentum resolution of the spectrometer is determined by the position resolution of the detectors and multiple scattering. Therefore the effects of the multiple scattering and the position resolution of the detectors are carefully considered in the Monte Carlo calculation. The corrections of the multiple scattering have been considered at the positions of MWPC, MWDC1 and MWDC2 in the computing program.

5. RESULTS

The momentum spectrum and angular spread $\Delta\theta_2$ of the particles with P = 800 MeV/*c* were calculated at the central momentum P_0 = 800 MeV/*c* and α = 30°. The results are shown in Fig. 2. From Fig. 2 we get ΔP (FWHM) ≈ 1.9 MeV, corresponding to the

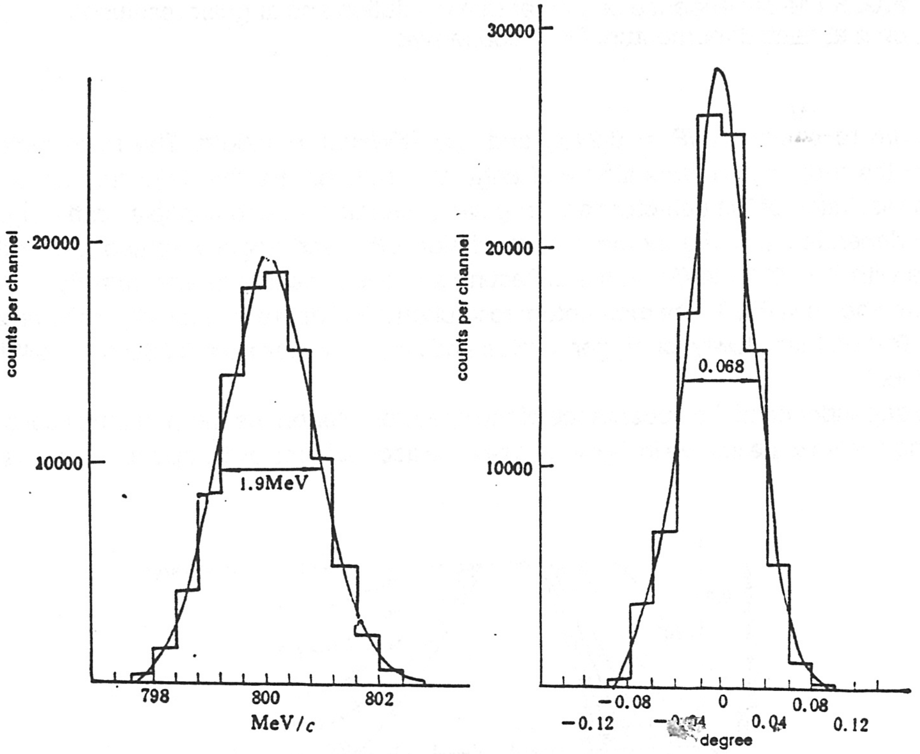

FIG. 2 The momentum spectrum and angular spread of the particles with P = 800 MeV/*c* (P_0 = 800 MeV/*c*, α = 30°).

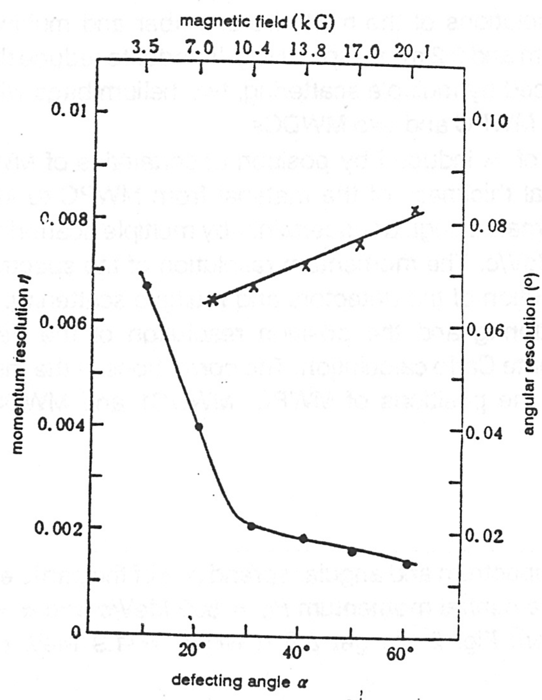

FIG. 3 The dependence of momentum resolution and angular resolution on α at central momentum $P_0 = 800$ MeV/c.

momentum resolution $\Delta P/P \approx 0.24\%$, and $\Delta\theta_2$ (FWHM) $\approx 0.068°$. The main factors affecting the momentum resolution and angular resolution are the deflecting angle α, position resolution of the detectors and angular uncertainty due to multiple scattering.

The dependence of the momentum resolution $\Delta P/P$ and angular spread $\Delta\theta_2$ of the particles with $P = 800$ MeV/c on the deflecting angle α at central momentum $P_0 = 800$ MeV/c are shown in Fig 3. The momentum resolution $\Delta P/P$ decreases rapidly in the range of $\alpha = 10°–30°$, then slowly for bigger α value and $\Delta\theta_2$ increases from 0.068° to 0.084° for $\alpha = 30°–60°$.

The dependence of the acceptance of the spectrometer on the momentum at several deflecting angles α are shown in Fig. 4. The relative acceptances of the spectrometer have

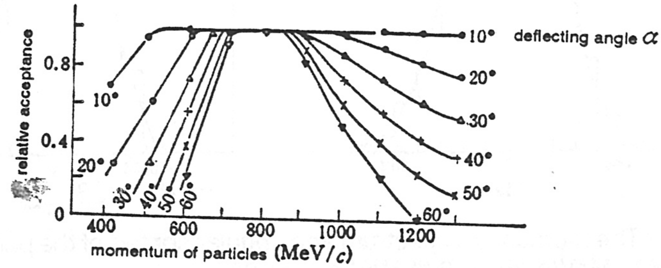

FIG. 4 The dependence of acceptance on momentum of particles ($P_0 =$ 800 MeV/c).

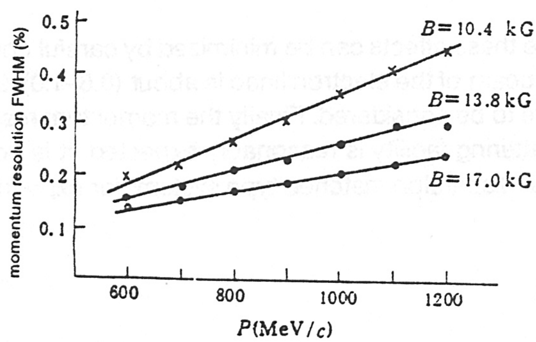

FIG. 5 The dependence of momentum resolution on momentum of particles at a certain magnetic field.

a rapid descent from 1 to zero at lower momentum region, but a rather slow descent at higher momentum region. A proper decrease of the size of the drift chamber MWDC2 can make a rapid descent of relative acceptance at higher momentum region and remain unchanged in lower and medium momentum region.

In a certain magnetic field the deflecting angle α' depends on the momentum of the particle, thus the momentum resolution $\Delta P/P$ also depends on the momentum of the particle. Fig. 5 shows the dependence of the momentum resolution on the momentum of the particles in a certain magnetic field.

The characteristics of the spectrometer are summarized in Table 1 according to the above results. Such a spectrometer is good enough for electron scattering experiments as described in section 1.

6. DISCUSSION

In our calculations we neglected the error caused in the installation of the spectrometer to the angles of β_1, β_2 and α and to the positions of the optical axis. We also neglected the effects of the momentum loss of the particle through the spectrometer. After all these factors are considered, the actual momentum resolution will not be as good as

TABLE 1.
The Characteristics of the Spectrometer (at central momentum P_0 = 800 MeV/c)

deflecting angle α		10°	20°	30°	40°	50°	60°
magnetic field B (KG)		3.5	7.0	10.4	13.8	17.0	20.1
momentum resolution $\frac{\Delta P}{P}$	P = 800 MeV/c	0.69%	0.40%	0.24%	0.19%	0.16%	0.14%
	P = 600—1200 MeV/c			(0.2—0.44)%	(0.15—0.26)%	(0.13—0.24)%	
angular spread $\Delta\theta_2$				0.068°	0.072°	0.076°	0.084°
P_{max}/P_{min}				2.5	2	1.7	1.6

the above results. Of cause these effects can be minimized by careful corrections. But the momentum spread of the beam of the electron linac is about (0.6–1.0)%, in addition , the effects from the target have to be considered. Finally the momentum resolution of (1–2)% for the whole electron scattering facility is reasonably expected. It is possible to rebuild the transport system into a "dispersion matched type system" for experiments with higher resolution.

ACKNOWLEDGEMENTS

Thanks are due to Mr. Liu Jiming for some work in his graduate study and thanks are also extended to Dr. Wang Zihua, Dr. Hou Xiaojiang and Mr. Zhang Qinjian for their interesting discussions.

REFERENCES

[1] Institute of High Energy Physics, Chinese Academy of Sciences, The preliminary design of the 2.2–2.8 GeV Electron-Positron Collider. Nov. 1982.
[2] Mao Zhenlin, the preparation studies of electron scattering in the medium and high energy range. Report on science foundation application of the Chinese Academy of Sciences. (1985.4).
[3] R. Auderson et. al., Nucl. Instru. and Math. 66 (1968) 328; H. Ehrenberg et. al., Nucl. Instru. and Math. 105 (1972) 253; P. Leconte et. al., Nucl. Instru. and Math. 169 (1980) 401.
[4] W. Bertozzi et al., Nucl. Instru. and Math. 162 (1979) 211.
[5] Luke Mo et al., SLAC * TN-69-29; SLAC-TN-65-40.
[6] K. L. Brown, SLAC Report, NO. 75 (1972).
[7] Liu Jiming, Mao Zhenlin, High Energy Physics and Nuclear Physics 9 (1985) 526.
[8] H. Enge, "Focusing of Charged Particles" Vol. 2.